Title

Finding the Fingerprint of Anthropogenic Climate Change in Marine Phytoplankton Abundance

Journal

Current Climate Change Reports, 6(2)

ISSN

2198-6061

Authors

Elsworth, Geneviève W
Lovenduski, Nicole S
McKinnon, Karen A
et al.

Publication Date

2020-06-01

DOI

10.1007/s40641-020-00156-w

Peer reviewed

Finding the Fingerprint of Anthropogenic Climate Change in Marine Phytoplankton Abundance

Geneviève W. Elsworth, Nicole S. Lovenduski, Karen A. McKinnon, Kristen M. Krumhardt & Riley X. Brady

Current Climate Change Reports

e-ISSN 2198-6061
Volume 6
Number 2

Curr Clim Change Rep (2020) 6:37-46
DOI 10.1007/s40641-020-00156-w

Springer

Current Climate Change Reports (2020) 6:37–46
https://doi.org/10.1007/s40641-020-00156-w

CARBON CYCLE AND CLIMATE (K ZICKFELD, JR MELTON AND N LOVENDUSKI SECTION EDITOR)

Finding the Fingerprint of Anthropogenic Climate Change in Marine Phytoplankton Abundance

Geneviève W. Elsworth[1] · Nicole S. Lovenduski[2] · Karen A. McKinnon[3] · Kristen M. Krumhardt[4] · Riley X. Brady[2]

Published online: 27 March 2020

Abstract

Purpose of Review We review how phytoplankton abundance may be responding to the increase in stratification associated with anthropogenic climate change, providing context on the utility of remote sensing datasets and Earth system model output to understand these perturbations.

Recent Findings Assessing disruption in the ocean biosphere using remote sensing datasets is challenged by the relatively short length of the observational record, restricting our ability to disentangle fluctuations due to internal climate variability from those imposed by externally forced anthropogenic trends. Ensembles of Earth system models can be used to quantify past and future drivers, but may not skillfully predict observed spatial patterns and temporal dynamics in marine phytoplankton.

Summary To better understand the role of internal climate variability in the observational record, we construct a synthetic ensemble of global chlorophyll concentration over the MODIS satellite mission using statistical emulation techniques. We emphasize the use of a synthetic ensemble to illuminate the role of internal climate variability in the evolution of the ocean biosphere over time.

Keywords Ocean biosphere · Phytoplankton abundance · Climate variability · Anthropogenic trends · Stratification · Global carbon cycle

Introduction

The ocean biosphere is an important component of the climate system, absorbing 30% of anthropogenic carbon emissions and storing 45× more carbon than the atmosphere [1]. Although phytoplankton constitute a small reservoir of carbon (3GtC), their capacity to photosynthetically fix carbon from the atmosphere enhances the ocean's role as a carbon sink [2]. The efficiency and strength of carbon sequestration by the biological pump in the oceanic reservoir strongly influences atmospheric carbon dioxide concentrations, with important feedbacks on the climate system [3, 4].

As the climate changes, the abundance and distribution of phytoplankton in the global ocean will likely also change. Increasing global temperatures will warm the ocean surface more than the ocean interior, driving an increase in ocean stratification [5]. An increase in stratification will reduce the upward flux of nutrients to the surface ocean and restrict phytoplankton growth, but may also alleviate light limitation [6, 7]. In contrast, colder, nutrient-rich regions may see an increase in phytoplankton growth as increasing temperatures stimulate phytoplankton metabolism [8, 9••].

Here, we review how phytoplankton abundance may be responding to the increase in stratification associated with anthropogenic climate change, providing context on the utility of remote sensing datasets and Earth system model (ESM)

This article is part of the Topical Collection on *Carbon Cycle and Climate*

✉ Geneviève W. Elsworth
genevieve.elsworth@colorado.edu

[1] Department of Geological Sciences and Institute of Arctic and Alpine Research, University of Colorado Boulder, Campus Box 450, Boulder, CO 80309-0450, USA

[2] Department of Atmospheric and Oceanic Sciences and Institute of Arctic and Alpine Research, University of Colorado Boulder, Boulder, CO, USA

[3] Department of Statistics and Institute of the Environment and Sustainability, University of California Los Angeles, Los Angeles, CA, USA

[4] Climate and Global Dynamics Laboratory, National Center for Atmospheric Research, Boulder, CO, USA

output to understand these perturbations. An ESM is a global climate or general circulation model (GCM) with explicit and interactive representation of terrestrial and marine carbon cycles and other biogeochemically important processes. Each of these methods has advantages and disadvantages in diagnosing anthropogenic change. Assessing disruption in the ocean biosphere using remote sensing datasets is challenged by the relatively short length of the observational record, restricting our ability to disentangle fluctuations due to internal climate variability from those imposed by externally forced anthropogenic trends [10]. While ensembles of ESMs can be used to quantify past and future changes in phytoplankton abundance and attribute these changes to internal or external drivers, models may not skillfully predict the observed phytoplankton chlorophyll field [9••, 11].

To overcome these limitations, we construct a synthetic ensemble of global ocean chlorophyll concentration by applying statistical emulation techniques to the 17-year Moderate Resolution Imaging Spectroradiometer (MODIS) chlorophyll record. Much like large initial condition ensembles generated with ESMs, our synthetic ensemble represents multiple possible evolutions of ocean chlorophyll concentration, each with a different phasing of internal climate variability (e.g., El Niño Southern Oscillation, Pacific Decadal Oscillation) but with shared external forcing (e.g., slow declines driven by increasing stratification) [12, 13, 14••]. Our synthetic ensemble can be used for a variety of purposes, including diagnosing patterns of internal variability in observed chlorophyll, and validating ESM representation of such variability.

Importance of Phytoplankton to Ocean Biogeochemical Dynamics

The distribution and abundance of phytoplankton in the global ocean is controlled by temperature and the availability of light and nutrients [15]. These variables are modulated by physical, chemical, and biological processes that vary across regional ocean ecosystems. The distribution of phytoplankton at a global scale can be quantified by the remote measurement of ocean color, specifically the reflectance of the photosynthetic pigment chlorophyll *a*. Chlorophyll concentration varies spatially and temporally by orders of magnitude across the global ocean (Fig. 1a). Variations in chlorophyll concentration may be attributed to changes in the physical environment, as well as phytoplankton physiology [16••]. Annual-mean chlorophyll concentration is elevated in the subpolar, polar, equatorial, and eastern boundary upwelling regions; high concentrations in these regions result from the upwelling of deep, nutrient-rich waters to the surface ocean. In contrast, regions such as the subtropical gyres display relatively lower chlorophyll concentrations due to restrictions in nutrient supply (Fig. 1a).

The global distribution of chlorophyll is also tightly coupled to light availability. Mean annual light availability decreases from the equator to the poles. In nutrient-replete subpolar and polar regions, phytoplankton growth is restricted in the winter when light is limited and enhanced in the spring, summer, and autumn when light is more abundant, creating a strong seasonal cycle in chlorophyll. In contrast, subtropical oceanic regions with ample light tend to be instead limited by the supply of nutrients due to a permanent thermocline, showing only moderate seasonality [17, 18]. Thus, the spatiotemporal distribution of chlorophyll in the global ocean varies primarily as a function of both light and nutrient availability. Further, satellite-derived chlorophyll measurements are frequently used in combination with other ocean variables (e.g., mixed layer depth, sea surface temperature) to estimate depth integrated net primary production (NPP) of ocean phytoplankton [19]. While various NPP algorithm solutions differ substantially, these aim to relate ocean color observations of chlorophyll to oceanic carbon cycling.

Phytoplankton harvest light to convert inorganic carbon to organic carbon through the process of photosynthesis. Oxygenic photosynthesis by phytoplankton in the surface ocean (between 0 and 200 m depth) is responsible for the consumption of carbon dioxide and the biochemical production of organic matter [20]. A high proportion (~ 99%) of this organic matter is respired by heterotrophic organisms in the surface ocean rather than exported to depth [21]. The sinking of a small fraction of organic carbon through the water column forms the basis of the biological pump, a biologically driven process which sequesters carbon from the atmosphere to the ocean interior [3]. The efficiency and strength of the biological pump strongly influences the global carbon cycle by contributing to the amount of carbon removed from the surface ocean and transported to depth [20].

The consumption of nutrients by phytoplankton influences the concentration and distribution of chemical species in the global ocean. When phytoplankton photosynthetically fix carbon in the surface ocean, they require a variety of nutrients. Nitrate, phosphate, and iron are among the nutrients required by phytoplankton and the assimilation of these nutrients in the surface ocean alters their vertical and lateral distribution [20]. Nutrients such as nitrate, phosphate, and silicate are considered macronutrients, which are required by phytoplankton in large amounts to support cellular growth and metabolism. In contrast, micronutrients such as iron, zinc, and cobalt are required in small amounts for the activity of enzymes and other intracellular functions [22]. In the global ocean, phytoplankton can be limited by either macronutrients or micronutrients. In polar regions, particularly the Southern Ocean, phytoplankton are limited by micronutrients, such as iron, and there is an abundance of macronutrients [23]. In contrast, in regions of the subtropical gyres, phytoplankton are limited by low concentrations of macronutrients such as nitrate and phosphate.

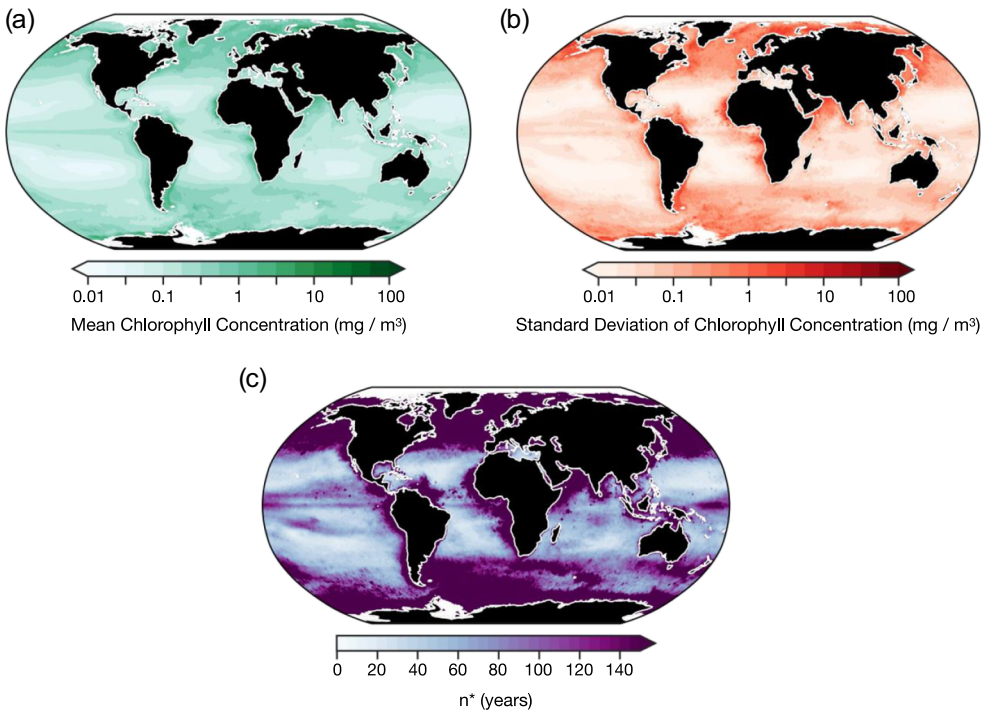

Fig. 1 **a** Spatial distribution of chlorophyll concentration in milligrams of carbon per cubic meter over the MODIS satellite record (2002 to 2019). **b** Standard deviation of detrended and deseasonalized chlorophyll concentration over the MODIS satellite record (2002 to 2019). **c** Number of years of continuous ocean color data required to distinguish a climate change driven trend in chlorophyll concentration from natural climate variability over the MODIS satellite record. Calculated following the method of Tiao et al. (1990) and Weatherhead et al. (1998)

In addition to influencing nutrient and carbon distributions in the ocean, phytoplankton also serve as the base of the marine food web [2]. Heterotrophic zooplankton graze on phytoplankton and act as primary consumers in oceanic ecosystems. Phytoplankton productivity supports complex food webs and diverse marine ecosystems by providing sustenance for higher trophic levels. Perturbations to phytoplankton productivity by anthropogenic climate change have the potential to trigger trophic cascades, dramatic reorganizations of the marine food web [24, 25]. However, the exact manifestations of these dramatic reorganizations in the ocean biosphere remain uncertain.

Anthropogenic Stratification and Ocean Phytoplankton

Anthropogenic climate change is heating the global ocean [5]. Due to direct contact with a warming atmosphere, the ocean's surface is warming more rapidly than deeper waters, with temperatures in the upper 75 m increasing at a rate of 0.11 °C per decade [26]. As a result, the thermal stratification (the strength of the vertical density gradient) of the upper ocean (0 to 200 m depth) has increased by approximately 4% since the 1970s, shoaling the depth of the mixed layer [26].

Enhanced stratification of the upper ocean restricts the transport of nutrients to the euphotic zone, limiting phytoplankton growth [6]. This trend is corroborated by both remote sensing datasets and ESM output. Remote sensing datasets suggest low-nutrient regions have expanded at rates of 0.8 to 4.3% per year between 1998 and 2006, consistent with a reduction in nutrient availability due to enhanced stratification [27, 28]. A variety of ESMs predict a reduction in net primary productivity (NPP) in low- to mid-latitude regions under twenty-first century global warming simulations [6, 8, 9••, 29–31, 32•, 33••]. The primary mechanism explaining this change is enhanced stratification and the subsequent restriction in vertical nutrient supply.

Observing Changes in Ocean Phytoplankton

Particles in the ocean, such as the photosynthetic pigment chlorophyll *a*, can absorb and scatter sunlight, altering the ocean's color. This color can be remotely observed by satellite imaging radiometers which measure the wavelength and intensity of any reflected electromagnetic radiation [34]. Chlorophyll reflects identifiable wavelengths and intensities, which can be used to infer certain phytoplankton properties and activities [35, 36]. Fluctuations in the relative intensity of the blue and green bands are driven by both changes in phytoplankton abundance in the surface water column and physiological responses to light and nutrient levels, allowing changes in the ocean biosphere to be observed on a variety of spatial and temporal scales [16••]. Although the reflected signal may provide incomplete spatial coverage due to obscuring clouds and sun glint, 8-day and longer composites constructed from daily datasets which incorporate an atmospheric correction provide a near-complete image [37].

Algorithms which convert ocean color to phytoplankton chlorophyll *a* concentration (mg m^{-3}) have evolved from simple empirical regressions [38] to complex radiative transfer equation inversions [39]. While each approach can be applied to a specific range of conditions, historically an algorithm based on the spectral ratio of remote sensing reflectance has been used to produce global chlorophyll *a* products from measurements made remotely by satellites. A commonly used algorithm to generate chlorophyll *a* products is the ocean color index (OCI), which measures the difference between reflectance measured in the green wavelengths and a linear reference between the blue and red wavelengths [40]. The OCI is particularly effective in the measurement of chlorophyll concentration below 0.25 mg m^{-3} which constitutes approximately three quarters of the global ocean [40]. These areas of relatively low chlorophyll concentration are concentrated in regions of the oligotrophic open ocean. Over the past several decades geospatial datasets of chlorophyll concentration have been generated by multiple satellite instruments with varying spatial and temporal coverage. These include the Coastal Zone Color Scanner (CZCS), the Ocean Color and Temperature Sensor (OCTS), the Sea-viewing Wide Field-of-view Sensor (SeaWiFS), the Moderate Resolution Imaging Spectroradiometer (MODIS), the Medium Resolution Imaging Spectrometer (MERIS), and the Visible Infrared Imaging Radiometer Suite (VIIRS). The MODIS satellite mission provides the longest continuous record of global ocean chlorophyll concentration, with coverage from 2002 to present. Figure 1a illustrates the mean of monthly averaged surface ocean chlorophyll concentrations calculated using the OCI algorithm at 1° × 1° resolution over the MODIS satellite mission (2002 to 2019).

Although there is a mechanistic understanding of how anthropogenic change may affect the ocean biosphere over time, there is debate about whether these changes are already detectable from remotely sensed observations [10, 41, 42, 43••, 44]. Assessing changes in the ocean biosphere using remote sensing data is challenged by the relatively short length of the continuous observational record and high temporal variability [41, 43••]. Figure 1b displays the standard deviation of monthly averaged surface ocean chlorophyll concentrations at 1° × 1° resolution from the MODIS record, illustrating that in addition to the spatial variability in chlorophyll (Fig. 1a), there is also substantial temporal variability.

The short length of the observed chlorophyll record restricts our ability to disentangle fluctuations due to internal climate variability from those imposed by externally forced anthropogenic trends [41, 43••]. In this context, *internal variability* refers to variability of the climate system which occurs in the absence of external forcing, and includes processes related to the coupled ocean-atmosphere system (e.g., El Niño Southern Oscillation (ENSO), Pacific Decadal Oscillation (PDO)) [45–47]. *External forcing*, in contrast, refers to the signal imposed by processes external to the climate system, such as solar variability, volcanic eruptions, and rising greenhouse gas concentrations from fossil fuel combustion [12, 46, 48]. While not all external forcing is *anthropogenic*, the long-term rise in global temperature that leads to stratification and possible declines in chlorophyll concentration is anthropogenic, rather than *natural* [26].

A small number of studies suggest that the influence of anthropogenic global warming on the ocean biosphere can be detected over an observational period as short as a decade [49]. A decline in global chlorophyll concentration by 0.01 Tg $year^{-1}$ between 1999 and 2006 was inferred by Behrenfeld et al. (2006) to reflect a response of the ocean biosphere to global climate change. An inverse relationship between chlorophyll concentration and sea surface temperature in the tropics and subtropics suggested that enhanced thermal stratification was restricting surface nutrient supply and limiting phytoplankton growth in these regions. Several recent studies using remote-sensing datasets have identified changes in satellite-derived chlorophyll or phytoplankton productivity in specific oceanic regions, such as the Southern Ocean [50•], and the Pacific and Indian Oceans [51••].

Studies of phytoplankton biomass or productivity over longer timescales have also attributed changes in phytoplankton abundance to anthropogenic climate change [52, 53•]. An integrated dataset of remote sensing observations and in situ chlorophyll measurements compiled since 1899 revealed a decrease in phytoplankton biomass by approximately 1% per year, attributable to enhanced thermal stratification [52]. However, observational datasets from the Hawaii Ocean Time Series (HOTS), Bermuda Atlantic Ocean Time Series (BATS), and the California Cooperative Oceanic Fisheries Investigations (CalCOFI) indicated increased phytoplankton biomass over the last 20 to 50 years [54]. These conflicting findings demonstrate the sensitivity of phytoplankton trends to the methodology and length of record.

A majority of studies which incorporate a variety of ESMs and remotely sensed datasets of phytoplankton abundance suggest that a continuous observational record of between 20 and 60 years is required to detect a statistically significant trend in remote sensing datasets of chlorophyll concentration [10, 41, 42, 43••, 55]. Long-term changes in the ocean biosphere are detectable if the trend is appreciably larger than the noise generated by internal climate variability and a sufficient length of continuous observations is available. However, in the majority of the global ocean the expression of internal variability obscures identification of possible forced secular trends in the climate record. The duration of observational time-series required varies regionally in the global ocean as a function of the regional secular signal to noise ratio [10]. The number of years required to distinguish a trend from

variability is calculated using the method of Tiao et al. (1990) and Weatherhead et al. (1998) [56, 57]. The number of years, n^*, required to detect a linear trend with a probability of 90% is

$$n^* = \left[\frac{3.3\sigma_N}{|\omega|}\sqrt{\frac{1+\varphi}{1-\varphi}}\right]^{2/3} \quad (1)$$

where σ_N is the standard deviation of the noise (chlorophyll anomalies with linear trend and seasonal cycle removed), ω is the trend (the global average trend in chlorophyll concentration over the observational period), and φ is the autocorrelation (the lag-1 autocorrelation of chlorophyll anomalies over the observational period). Figure 1c illustrates the number of years of continuous remote sensing data required to distinguish a trend in chlorophyll concentration from variability over the MODIS satellite mission. The length of the time series required to detect a statistically significant trend varies regionally, with relatively short time series required in regions with low temporal variability (subtropics) and relatively longer time series required in regions with high temporal variability (coastal upwelling zones and polar regions).

Using Eq. 1, with σ_N and φ estimated from satellite observations at 1° × 1° resolution, we find approximately 40 years of continuous remote sensing observations are required to detect a statistically meaningful trend in global chlorophyll concentrations, while detection times are predicted to be shorter (20 to 30 years) in regions with relatively lower temporal variability (Fig. 1c) [10]. This is in agreement with previous modeling studies which also used Eq. 1 to determine detection timescales for anthropogenic changes in surface chlorophyll concentrations but estimated the parameter values with ESMs [43••].

Modeling Changes in Ocean Phytoplankton

Earth system models (ESMs) can be used as a predictive tool to identify long-term changes in phytoplankton abundance and productivity under different emission scenarios. In simulations under twenty-first century global warming conditions, phytoplankton abundance is predicted to decrease globally [8, 30, 58]. Most models included in the Coupled Model Intercomparison Project Phase 5 (CMIP5) show consistent declines in phytoplankton abundance by 2100, though the magnitude of the decrease varies substantially between models [8, 59]. The majority of models project an increase in phytoplankton abundance in the high latitude ocean as light limitation is alleviated from thermal stratification, increasing temperature stimulates photosynthesis, and sea ice cover declines. In contrast, a decrease in the low latitude oceans is projected as nutrient limitation from thermal stratification is enhanced [8, 30, 33••].

A warming ocean can both enhance phytoplankton growth rate as increased temperatures accelerate metabolic reactions and restrict phytoplankton abundance due to enhanced thermal stratification resulting in surface nutrient reductions [31]. These conflicting controls on phytoplankton growth may generate regional differences in simulated phytoplankton abundance projections depending on the predominant effect [31, 32•]. For example, in CMIP5 models, integrated phytoplankton abundance projections with climate change vary latitudinally depending on whether temperature, light, micronutrients, or macronutrients are limiting, with macronutrient and temperature controls dominant between 45°S to 45°N latitude [60].

Regional biome changes under climate warming scenarios are also predicted to shift phytoplankton community structure. Thermal stratification and subsequent nutrient reduction are predicted to favor the success of small phytoplankton relative to large phytoplankton [61, 62]. Due to a relatively larger surface area-to-volume ratio, smaller phytoplankton more efficiently assimilate nutrients than larger phytoplankton. The parameterization of this effect in the Community Earth System Model (CESM) generates biogeochemical regime boundaries at 45°N and 45°S latitude, where a specific threshold surface nutrient concentration occurs; within the low-latitude region demarcated by these boundaries, decreases in surface nutrient supply result in greater decreases in large phytoplankton biomass because smaller phytoplankton are less impacted by nutrient decreases in low-nutrient conditions [61].

A relatively new approach to distinguishing externally forced anthropogenic signals from internal climate variability in modeled ocean phytoplankton is to analyze output from an ensemble of simulations conducted with a single Earth system model; here, each ensemble member has a different phasing of internal variability, but shares identical external forcing with other ensemble members [12]. An ensemble of simulations which each differ slightly in their initial conditions generates large internal variability in ocean biogeochemical variables, while the ensemble mean demonstrates externally forced trends [63–68, 69••]. The Community Earth System Model large ensemble (CESM-LE) is a fully coupled global climate model that provides reconstructions of Earth's past climate and projections of Earth's future climate under different forcing scenarios, simulating the temporal evolution of the climate system of multiple ensemble members, each with slightly different initial conditions [70]. Many other fully coupled climate models also utilize the large ensemble framework, including the GFDL Earth System Model 2M (ESM2M) [63, 67, 69••].

In order to quantify timescales over which externally forced trends in multiple ocean biogeochemical variables can emerge from internal variability, Rodgers et al. (2015) employed a perturbed initial condition ensemble of ESM2M to simulate changes under a historical emission

scenario and representative concentration pathway 8.5 (RCP 8.5), which is considered a high emissions or business-as-usual scenario [63]. This analysis revealed that anthropogenic changes to global mean marine NPP would be the last of four biogeochemical variables analyzed to emerge from internal variability after changes in acidification, SST, and oxygen concentrations, respectively. A complementary study with the same model framework that incorporated several additional biogeochemical variables also found that global warming-induced changes in marine NPP would be slowest to emerge [69••]. Taken together, these two studies suggest that significant changes in phytoplankton biomass may take a longer time to detect compared with other biogeochemical variables [63, 69••].

In addition to diagnosing timescales of emergence for biogeochemical parameters, perturbed initial condition ensembles can be used to constrain the contribution of internal climate variability on uncertainty in projections of marine NPP. Simulations forced with radiative forcing scenarios RCP 2.6 and RCP 8.5 using CMIP5 models revealed that internal climate variability in ESMs can contribute significant uncertainty to future projections of marine NPP, especially on regional scales [9••, 67]. Krumhardt et al. (2017) identified avoidable impacts of anthropogenic climate change on declining phytoplankton abundance by comparing ensemble integrations of the CESM-LE forced with two different radiative forcing scenarios: RCP 4.5 (mitigation emission scenario) and RCP 8.5 (high emissions scenario) [9••]. Their study suggests that if we follow a mitigation emission scenario (RCP 4.5), large-scale regional declines in NPP are only avoidable in the Atlantic sector, whereas large internal climate variability precludes statistical separation of the externally forced NPP response elsewhere.

Although ESMs are an effective tool for projecting the response of the ocean biosphere to anthropogenic climate change, it is essential to consider how the ESM representation of phytoplankton abundance compares to observed records of phytoplankton over time. Phytoplankton concentrations have been measured continuously over multiple decades at several ocean time series locations in the global ocean. Saba et al. (2010) compared the representation of chlorophyll concentration from 36 ESMs with embedded biogeochemistry to observational datasets collected at the ocean time series of HOTS and BATS between 1989 and 2007 [54]. At both sites, time-series observations of monthly mean chlorophyll concentration are larger than those produced by 90% of current generation ESMs, motivating further evaluation of the ESM representation of chlorophyll on both monthly and interannual timescales; the models also performed relatively poorly at producing an observed increasing NPP trend, indicating that ESMs may not accurately simulate multiannual changes in phytoplankton abundance over short time periods.

Synthetic Ensemble of Ocean Chlorophyll Concentration

A complementary approach to quantifying internal variability in phytoplankton abundance is to construct an observationally constrained synthetic ensemble by statistically emulating the satellite-derived chlorophyll record. Observations can provide a strong constraint on uncertainty related to internal climate variability over time in cases where the dominant timescales of variability are resolved within the observed record. With this constraint, the synthetic ensemble consists of alternate evolutions of the observed spatiotemporal field that preserve the statistical properties of the single observational record.

In order to generate a synthetic ensemble of global chlorophyll concentration, we build upon the statistical model developed in McKinnon et al. (2017) and McKinnon and Deser (2018) for temperature, precipitation, and sea level pressure [13, 14••]. In our case, we model chlorophyll concentration as

$$X^{i,t} = \beta_o^i + \beta_S^{i,t} + \beta_F^t + \beta_{\mathrm{ENSO}}^i M_{\mathrm{ENSO}}^t + \beta_{\mathrm{PDO}}^i M_{\mathrm{PDO}}^t + \varepsilon^{i,t} \quad (2)$$

where $X^{i,\,t}$ is the chlorophyll concentration at location i and time t. We model chlorophyll as a linear combination of the mean state (β_o^i), seasonality ($\beta_S^{i,t}$), response to external forcing (β_F^t), response to two dominant climate modes $\left(\beta_{\mathrm{ENSO}}^i M_{\mathrm{ENSO}}^t,\ \beta_{\mathrm{PDO}}^i M_{\mathrm{PDO}}^t\right)$, and residual internal climate variability ($\varepsilon^{i,\,t}$). Importantly, the β_F^t term in Eq. 2 represents the chlorophyll response to external forcing, while the last three terms represent internal climate variability. The two time series M_{ENSO}^t and M_{PDO}^t represent the evolution of the climate modes ENSO and PDO respectively, which have been shown to influence chlorophyll concentration [71–73]. Due to covariance between ENSO and PDO, we have created two orthogonalized time series via principal component analysis of the original observed temporal evolution of ENSO and PDO over 1880 to 2019. Chlorophyll anomalies are calculated by removing the mean state (β_o^i), monthly climatology ($\beta_S^{i,t}$), and linear trend in global mean chlorophyll (β_F^t) from the original MODIS dataset of chlorophyll concentration at monthly, 1° × 1° resolution (Fig. 2b). β_{ENSO}^i and β_{PDO}^i are estimated by calculating the ordinary least squares regression of the MODIS chlorophyll anomalies against time series of ENSO and PDO to determine the sensitivity of chlorophyll concentration to these modes. The spatially varying regression coefficients are multiplied by the observed indices and subtracted from the chlorophyll anomalies to remove the direct influence of the climate modes from the time series (Fig. 2b), leaving us with the residual internal climate variability, $\varepsilon^{i,t}$.

We take a two-step process to create the synthetic ensemble. First, the residuals, $\varepsilon^{i,t}$, are resampled 1000 times using the nonparametric moving block bootstrap (MBB) in time, retaining their spatial structure (Fig. 2c) [74]. The

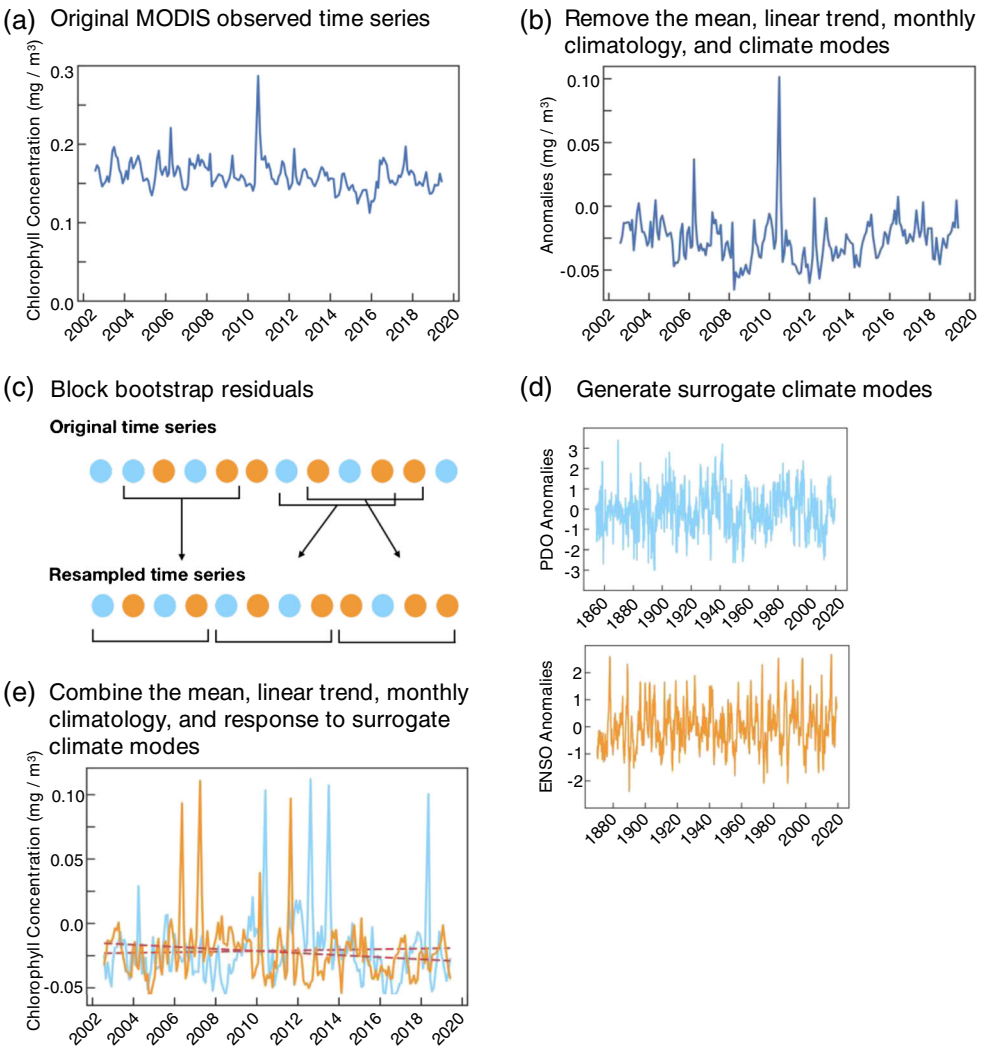

Fig. 2 Schematic representation of the construction of a synthetic ensemble of regional ocean chlorophyll concentration in the Eastern Equatorial Pacific. **a** Original MODIS observed time series. **b** Remove mean, linear trend, monthly climatology, and scaled climate modes from original time series. **c** Block bootstrap residuals 1000 times using the moving block bootstrap method. **d** Generate 1000 surrogate climate modes of ENSO and PDO using the iterative adjusted amplitude Fourier transformation method. **e** Generate distinct ensemble members by combining the mean, the trend, the seasonal cycle, the block bootstrapped anomalies, and the response to surrogate climate modes. Synthetic ensemble member 3 is shown in the light blue line, and synthetic ensemble member 10 is shown in the orange line. Dashed red lines represent the trend of each synthetic ensemble member over the observational period

residuals are resampled using a block length of 12 months which fully encapsulates the seasonal cycle in global chlorophyll concentration variability. Second, the response of chlorophyll concentration to different possible evolutions of climate modes over time is incorporated by generating 1000 surrogate climate modes of ENSO and PDO using the iterative adjusted amplitude Fourier transformation (IAAFT) method (Fig. 2d) [75, 76]. This surrogate data approach produces an ensemble of time series with the same spectral characteristics as the original climate mode time series. The surrogate climate modes are multiplied by the regression coefficients, β^i_{ENSO} and β^i_{PDO}, estimated from the observed record to create time series of chlorophyll that could have occurred given a different temporal evolution of ENSO and PDO. We combine the block bootstrapped anomalies and the response to the surrogate climate modes with β^i_o, $\beta^{i,t}_S$, and β^t_F to produce multiple distinct synthetic ensemble members (Fig. 2e). Figure 2e illustrates the temporal evolution of two synthetic ensemble members in the Eastern Equatorial Pacific. Each member displays a different long-term trend at this location due to different sampling of climate variability.

Figure 3 displays the spatial pattern of the trend in annual-mean chlorophyll concentration over 2002 to 2019 for two distinct synthetic ensemble members. Synthetic ensemble members 3 (Fig. 3a) and 10 (Fig. 3b) exhibit trends of opposite sign in many regions of the ocean. For example, in the Eastern Equatorial Pacific, synthetic ensemble member 3 depicts a trend toward increasing chlorophyll concentrations over time, while synthetic ensemble member 10 displays a trend toward decreasing chlorophyll. This behavior is also apparent in the California Current Eastern Boundary Upwelling System, the subpolar North Atlantic, the subtropical Pacific, and the Southern Ocean. Thus, results from our synthetic ensemble suggest that internal variability plays an important role in chlorophyll concentration in these regions, consistent with previous studies [10, 48, 69••].

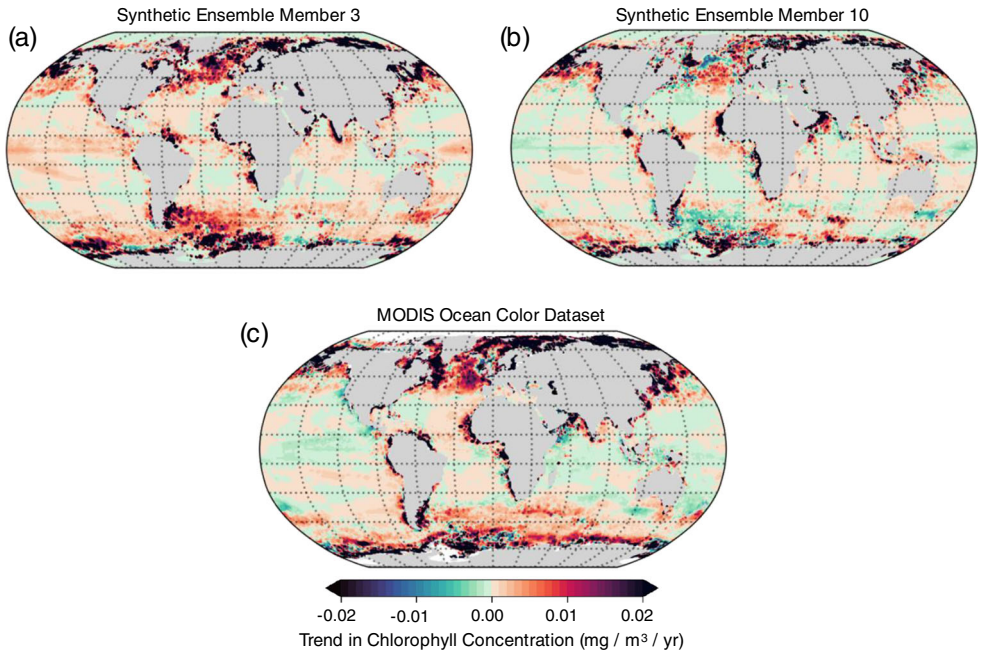

Fig. 3 **a** Annual trend in global chlorophyll concentration from 2002 to 2019 of synthetic ensemble member 3. **b** Annual trend in global chlorophyll concentration from 2002 to 2019 of synthetic ensemble member 10. **c** Annual trend in global chlorophyll concentration from 2002 to 2019 over the MODIS ocean color record

Observed trends in real-world chlorophyll concentration from the MODIS record (Fig. 3c) show decreasing chlorophyll over time in the subtropical oceans and the California Current Eastern Boundary Upwelling System, with increasing chlorophyll over time in the subpolar North Atlantic, parts of the Southern Ocean, and other Eastern Boundary Upwelling Systems. The real world is a single realization (or ensemble member) in our ensemble framework. As such, the observational record is equally affected by the phasing of internal climate variability in the real world. That the negative trend in observed chlorophyll in the California Current Eastern Boundary Upwelling System is captured in synthetic ensemble member 3 but not member 10 implies that the observed trend is driven by the phasing of internal variability, for example. Our synthetic ensemble thus cautions against interpreting trends as externally driven across much of the global ocean.

Conclusions

The abundance and distribution of phytoplankton in the global ocean are controlled by both internal climate variability and external anthropogenic forcing. Our understanding of the ocean biosphere has been informed by the analysis of remote sensing datasets and ESM output. Each of these methods has advantages and disadvantages to diagnosing changes in marine phytoplankton over time. Assessing disruption in the ocean biosphere using remote sensing datasets is challenged by the relatively short length of the observational record, restricting our ability to disentangle fluctuations in internal climate variability from externally forced anthropogenic trends. Ensembles of Earth system models can be used to confidently isolate the response due to internal climate variability and external forcing, but may not skillfully represent observed spatial patterns in marine phytoplankton.

To reconcile these differences between the satellite-derived observational record and ESM output, we implement the novel approach of constructing a synthetic ensemble of global chlorophyll concentration using data from the MODIS satellite mission. Our synthetic ensemble reveals an important role for internal variability in surface ocean chlorophyll across the global ocean. It further cautions against interpreting long-term trends from the observed record as driven by externally forced anthropogenic climate change.

Funding Information GWE, NSL, KMK, and RXB are funded by the National Science Foundation (OCE-1752724, OCE-1558225).

Compliance With Ethical Standards

Conflict of Interest The authors declare no competing financial interests.

References

Papers of particular interest, published recently, have been highlighted as:
- • Of importance
- •• Of major importance

1. Friedlingstein P, Jones MW, O'Sullivan M, et al. Global carbon budget 2019. Earth Syst Sci Data. 2019;11:1783–838.
2. Falkowski P. The power of plankton. Nature. 2012;483:S17–20.

3. McKinley GA, Fay AR, Lovenduski NS, Pilcher DJ. Natural variability and anthropogenic trends in the ocean carbon sink. Annu Rev Mar Sci. 2017;9:125–50.
4. Bindoff NL, Cheung WWL, Kairo JG, et al. Changing ocean, marine ecosystems, and dependent communities. In: Intergovernmental Panel on Climate Change 2019: Summary for Policymakers. 2019.
5. Levitus S, Antonov JI, Boyer TP, et al. Global ocean heat content 1955-2008 in light of recently revealed instrumentation problems. Geophys Res Lett. 2009;36:1–5.
6. Bopp L, Monfray P, Aumont O, et al. Potential impact of climate change on marine export production. Glob Biogeochem Cycles. 2001;15:81–99.
7. Lozier MS, Dave AC, Palter B, Gerber LM, Barber RT. On the relationship between stratification and primary productivity in the North Atlantic. Geophys Res Lett. 2011;38:L18609.
8. Bopp L, Resplandy L, Orr JC, et al. Multiple stressors of ocean ecosystems in the 21st century: projections with CMIP5 models. Biogeosciences. 2013;10:6225–45.
9.•• Krumhardt KM, Lovenduski NS, Long MC, Lindsay K. Avoidable impacts of ocean warming on marine primary production: Insights from the CESM ensembles. Glob Biogeochem Cycles. 2017;31:114–33 **This paper uses two ensembles of an Earth system model under different forcing scenarios to identify anthropogenic impacts on marine net primary production.**
10. Henson SA, Sarmiento JL, Dunne JP, et al. Detection of anthropogenic climate change in satellite records of ocean chlorophyll and productivity. Biogeosciences. 2010;7:621–40.
11. Doney SC, Lima I, Moore JK, et al. Skill metrics for confronting global upper ocean ecosystem-biogeochemistry models against field and remote sensing data. J Mar Syst. 2009;76:95–112.
12. Deser C, Philips A, Bourdette V, Teng H. Uncertainty in climate change projections: the role of internal variability. Clim Dyn. 2012;38:527–46.
13. McKinnon KA, Poppick A, Dunn-Sigouin E, Deser C. An "observational large ensemble" to compare observed and modeled temperature trend uncertainty due to internal variability. J Clim. 2017;30:7585–98.
14.•• McKinnon KA, Deser C. Internal variability and regional climate trends in an Observational Large Ensemble. J Clim. 2018;31:6783–802 **This paper generates a synthetic ensemble of temperature, precipitation, and global sea level pressure.**
15. Sigman DM, Hain MP. The biological productivity of the ocean. Nat Educ. 2012;3:1–16.
16.•• Behrenfeld M, O'Malley RT, Boss ES, et al. Revaluating ocean warming impacts on global phytoplankton. Nat Clim Chang. 2016;6:323–30 **This paper examines the influence of photoacclimation on phytoplankton intracellular chlorophyll concentrations.**
17. Lalli CM, Parsons TR. Phytoplankton and primary production. In: Biological oceanography: An introduction. Amsterdam: Elsevier Butterworth-Heinemann; 2006.
18. Giovannoni SJ, Vergin KL. Seasonality in ocean microbial communities. Science. 2012;335:671–6.
19. Saba VS, Friedrichs MAM, Antoine D, et al. An evaluation of ocean color model estimates of marine primary productivity in coastal and pelagic regions across the globe. Biogeosciences. 2011;8:489–503.
20. Sarmiento JL, Gruber N. Organic matter export and remineralization. In: Ocean Biogeochemical Dynamics. Princeton, Woodstock: Princeton University Press; 2006.
21. Emerson S, Hedges J. Life processes in the ocean. In: Chemical Oceanography and the Marine Carbon Cycle. Cambridge University Press; 2008.
22. Sunda WG. Trace metal interactions with marine phytoplankton. Biol Oceanogr. 2013;6:411–42.
23. Moore JK, Doney SC, Glover DM, Fung IY. Iron cycling and nutrient-limitation patterns in surface waters of the World Ocean. Deep-Sea Res II Top Stud Oceanogr. 2002;49:463–507.
24. Cheung WWL, Lam VWY, Sarmiento JL, et al. Large-scale redistribution of maximum fisheries catch potential in the global ocean under climate change. Glob Chang Biol. 2010;16:24–35.
25. Pörtner HO, Karl DM, Boyd PW, et al. Ocean systems. In: Climate Change 2014: Impacts, adaptation, and vulnerability. Part A: Global and Sectoral Aspects. Contribution of Working Group II to the Fifth Assessment Report of the Intergovernmental Panel on Climate Change.
26. Rhein M, Rintoul SR, Aoki S, et al. Observations: Ocean. In: Climate Change 2013: The physical science basis. Contribution of Working Group I to the Fifth Assessment Report of the Intergovernmental Panel on Climate Change.
27. Polovina JJ, Howell EA, Abecassis M. Ocean's least productive waters are expanding. Geophys Res Lett. 2008;35:2–6.
28. Irwin AJ, Oliver MJ. Are ocean deserts getting larger? Geophys Res Lett. 2009;36:1–5.
29. Schmittner A, Oschlies A, Matthews HD, Galbraith ED. Future changes in climate, ocean circulation, ecosystems, and biogeochemical cycling simulated for a business-as-usual CO_2 emission scenario until year 4000 AD. Glob Biogeochem Cycles. 2008;22:1–21.
30. Steinacher M, Joos F, Frölicher TL, et al. Projected 21st century decrease in marine productivity: a multi-model analysis. Biogeosciences. 2010;7:979–1005.
31. Marinov I, Doney SC, Lima ID, Lindsay K, Moore JK, Mahowald N. North-south asymmetry in the modeled phytoplankton community response to climate change over the 21st century. Glob Biogeochem Cycles. 2013;27:1274–90.
32.• Laufkötter C, Vogt M, Gruber N, et al. Drivers and uncertainties in future global marine primary production in marine ecosystem models. Biogeosciences. 2015;12:6955–6984.4 **This paper compares projected changes in marine net primary productivity in multiple Earth system under high-emission scenario RCP 8.5.**
33.•• Kwiatkowski L, Bopp L, Aumont O. Emergent constraints on projections of declining primary production in the tropical oceans. Nat Clim Chang. 2017;7:355–8 **This article integrates Earth system model projections and remotely sensed observations to constrain long-term trends in marine primary production.**
34. Neville RA, Gower JFR. Passive remote sensing of phytoplankton via chlorophyll a fluorescence. J Geophys Res. 1977;82:3487–93.
35. Meister G, Franz BA, Kwiatkowska EJ, McClain CR. Corrections to the calibration of MODIS Aqua ocean color bands derived from SeaWiFS data. IEEE Trans. 2012;60:310–9.
36. Siegel DA, Behrenfeld MJ, Maritorena S, et al. Regional to global assessments of phytoplankton dynamics from the SeaWiFS mission. Remote Sens Environ. 2013;135:77–91.
37. Feng L, Hu C. Cloud adjacency effects on top-of-atmosphere radiance and ocean color data products: a statistical assessment. Remote Sens Environ. 2016;174:301–13.
38. Gordon HR, Morel AY. Water algorithms. In: Remote Assessment of Ocean Color for Interpretation of Satellite Visible Imagery. New York: Springer-Verlag; 1983.
39. Maritorena S, Siegel DA, Peterson A. Optimization of a semi-analytical ocean color model for global scale applications. Appl Opt. 2002;41:2705–14.
40. Hu C, Lee Z, Franz B. Chlorophyll a algorithms for oligotrophic oceans: a novel approach based on three-band reflectance difference. J Geophys Res Ocean. 2012;117:1–25.
41. Beaulieu C, Henson SA, Sarmiento JL, et al. Factors challenging our ability to detect long-term trends in ocean chlorophyll. Biogeosciences. 2013;10:2711–24.
42. Henson SA. Slow science: the value of long ocean biogeochemistry records. Philos Trans R Soc. 2014;372:1-22.

43.•• Henson SA, Beaulieu C, Lampitt R. Observing climate change trends in ocean biogeochemistry: when and where. Glob Chang Biol. 2016;22:1561–71 **This article uses an ensemble of Earth system models to quantify timescales required to detect long-term trends in several biogeochemical variables**.

44. Hammond ML, Beaulieu C, Sahu SK, Henson SA. Assessing trends and uncertainties in satellite-era ocean chlorophyll using space-time modeling. Glob Biogeochem Cycles. 2017;31:1103–17.

45. Santer BD, Mears C, Doutriaux C, et al. Separating signal and noise in atmospheric temperature changes: the importance of timescales. J Geophys Res Atmos. 2011;116:1–19.

46. Deser C, Knutti R, Solomon S. Communication on the role of natural variability in future North American climate. Nat Clim Chang. 2012b;2:775–9.

47. Meehl GA, Hu A. Externally forced and internally generated decadal climate variability associated with the Interdecadal Pacific Oscillation. J Clim. 2013;26:7298–7310.

48. Schneider DP, Deser C. Tropically driven and externally forced patterns of Antarctic Sea ice change: reconciling observed and modeled trends. Clim Dyn. 2018;50:4099–618.

49. Behrenfeld MJ, O'Malley RT, Siegel DA, et al. Climate-driven trends in contemporary ocean productivity. Nature. 2006;444:752–5.

50.• Del Castillo CE, Signorini SR, Karaköylü EM, Rivero-Calle S. Is the Southern Ocean getting greener? Geophys Res Lett. 2019;46:6034–40. **This paper highlights regional increases in chlorophyll concentration in the Southern Ocean.**

51.•• Gregg WW, Rousseaux CS. Global ocean primary production trends in the modern ocean color satellite record (1998–2015). Environ Res Lett. 2019;14:1–9. **This paper assimilates ocean color data into an Earth system model to estimate changes in marine primary production.**

52. Boyce DG, Lewis MR, Worm B. Global phytoplankton decline over the past century. Nature. 2010;466:591–6.

53.• Osman MB, Das SB, Trusel LD, et al. Industrial-era decline in subarctic Atlantic productivity. Nature. 2019;569:551–5. **This paper integrates observational datasets in the Arctic to identify regional declines in productivity.**

54. Saba VS, Friedrichs MAM, Carr ME, et al. Challenges of modeling depth-integrated marine primary productivity over multiple decades: a case study at BATS and HOT. Glob Biogeochem Cycles. 2010;24:1–21.

55. Gregg WW, Rousseaux CS. Decadal trends in global pelagic chlorophyll: a new assessment integrating multiple satellites, in situ data, and models. J Geophys Res Oceans. 2014;119:5921–33.

56. Tiao GC, Reinsel GC, Xu D, et al. Effects of autocorrelation and temporal sampling schemes on estimates of trend and spatial correlation. J Geophys Res. 1990;95:507–20.

57. Weatherhead EC, Reinsel GC, Tiao GC, et al. Factors affecting the detection of trends: statistical considerations and applications to environmental data. J Geophys Res Atmos. 1998;103:17149–61.

58. Henson S, Cole H, Beaulieu C, Yool A. The impact of global warming on seasonality of ocean primary production. Biogeosciences. 2013;10:4357–69.

59. Cabré A, Marinov I, Leung S. Consistent global responses of marine ecosystems to future climate change across the IPCC AR5 Earth system models. Clim Dyn. 2015;45:1253–80.

60. Leung S, Cabré A, Marinov I. A latitudinally banded phytoplankton response to 21st century climate change in the Southern Ocean across the CMIP5 model suite. Biogeosciences. 2015;12:5715–34.

61. Marinov I, Doney SC, Lima ID. Response of ocean phytoplankton community structure to climate change over the 21st century: partitioning the effects of nutrients, temperature and light. Biogeosciences. 2010;7:3941–59.

62. Moore JK, Lindsay SC, Doney MC, Long MC, Misumi K. Marine ecosystem dynamics and biogeochemical cycling in the Community Earth System Model [CESM1(BGC)]: comparison of the 1990s with the 2090s under the RCP4.5 and RCP8.5 scenarios. J Clim. 2013;26:9291–312.

63. Rodgers KB, Lin J, Frölicher TL. Emergence of multiple ocean ecosystem drivers in a large ensemble suite with an earth system model. Biogeosciences. 2015;12:3301–20.

64. Long MC, Deutsch C, Ito T. Finding forced trends in oceanic oxygen. Glob Biogeochem Cycles. 2016;30:381–97.

65. McKinley GA, Pilcher DJ, Fay AR, Lindsay K, Long MC, Lovenduski NS. Timescales for detection of trends in the ocean carbon sink. Nature. 2016;530:469–72.

66. Lovenduski NS, McKinley GA, Fay AR, Lindsay K, Long MC. Partitioning uncertainty in ocean carbon uptake projections: internal variability, emission scenario, and model structure. Glob Biogeochem Cycles. 2016;30:1276–87.

67. Frölicher TL, Rodgers KB, Stock CA, Cheung WWL. Sources and uncertainties in 21st century projections of potential ocean ecosystem stressors. Glob Biogeochem Cycles. 2016;30:1224–43.

68. Brady RX, Lovenduski NS, Alexander MA, Jacox M, Gruber N. On the role of climate modes in modulating air-sea CO_2 fluxes in eastern boundary upwelling systems. Biogeosciences. 2019;16:329–46.

69.•• Schlunegger S, Rodgers KB, Sarmiento JL, et al. Emergence of anthropogenic signals in the ocean carbon cycle. Nat Clim Chang. 2019;9:719–25. **This paper identifies the emergence of marine net primary production the latest of several ocean biosphere stressors.**

70. Kay JE, Deser C, Phillips A, et al. The community earth system model (CESM) large ensemble project. Bull Am Meteorol Soc. 2015;96:1333–49.

71. Gregg WW, Conkright ME. Decadal changes in global ocean chlorophyll. Geophys Res Lett. 2002;29:1-4.

72. Yoder JA, Kennelly MA. Seasonal and ENSO variability in global ocean phytoplankton chlorophyll derived from 4 years of SeaWiFS measurements. Glob Biogeochem Cycles. 2003;17:1112.

73. Radenac M, Léger F, Singh A, Delcroix T. Sea surface chlorophyll signature in the tropical Pacific during eastern and central Pacific ENSO events. J Geophys Res. 2012;117:C04007.

74. Wilks DS. Resampling hypothesis tests for autocorrelated fields. J Clim. 1997;10:65–82.

75. Theiler J, Eubank S, Longin A, Galdrikian B, Farmer JD. Testing for nonlinearity in time series: the method of surrogate data. Phys D. 1992;58:77–94.

76. Schreibner T, Schmitz A. Surrogate time series. Phys D. 2000;142:346–82.